Real options in energy policy: the case for a market-based technology adoption

Frank Heinz[a], Reinhard Madlener[b,c,*]

[a] *RWTH Aachen University, Templergraben 55, 52066, Aachen, Germany*
[b] *Chair of Energy Economics and Management, Institute for Future Energy Consumer Needs and Behavior (FCN), School of Business and Economics / E.ON Energy Research Center, RWTH Aachen University, Mathieustrasse 10, 52074, Aachen, Germany*
[c] *Department of Industrial Economics and Technology Management, Norwegian University of Science and Technology (NTNU), Sentralbygg 1, Gløshaugen, 7491, Trondheim, Norway*

Abstract

The ongoing energy transition requires investment in electrolyzer capacity, very quickly, and on an industrial scale. Moreover, society expects this to happen in a cost-efficient manner. In this article, for the German market, we show that a market-based technology adoption is a realistic policy option to achieve both targets. We demonstrate this in two steps. First we show that by moving all power generation assets to the day-ahead market for electricity, this market continues to function also under the condition of a fully decarbonized economy. Second, we show that in such a market environment, investments in electrolyzers can be expected to pick up without incentives and delay.

Keywords: Real Options, Energy Transition, Day-ahead Market, Optimal Stopping, Decision Making under Uncertainty

JEL Classification Nos.: C61, C63, D81, G11, Q41, Q48

1. Introduction

The European Union plans to decarbonize until the year 2050 at the latest (European Commission 2019). While the technology for this transition is well advanced, the energy policy for adopting the technology is criticized as inadequate (e.g., Sokołowski and Heffron 2022), or, ref. Hanny et al. 2022). In this article we analyze the possibility of a market-based technology adoption by presenting he show-case of an electrolyzer retrofit to an offshore wind farm. Electrolyzers are one of the different components which are needed for a successful decarbonization on an industrial scale, like storage and backup power. Currently, in this technology, we see only little progress –

*Corresponding author.
E-mail address: RMadlener@eonerc.rwth-aachen.de (R. Madlener).

e.g., for Germany, the National Academy of Science and Engineering (2023) lists ca. 250 MW of operating electrolyzers, and additionally ca. 550 MW under construction. At the same time, e.g., ISE (2021) estimates that a capacity of 40 - 160 GW will be needed by 2045, and other studies pointing at a similar order of magnitude. Also internationally, the development is too slow to reach the energy transition targets; for this reason, the International Energy Agency recommends support schemes urgently (IEA 2023). For policy makers, the question therefore arises, which market regulation triggers such investments on a large scale, quickly and efficiently?

To ensure efficiency, a market-based approach is preferable over subsidies. Two arguments are often presented against this. At one, there is concern that the day-ahead market for electricity, which is the most important place for competition, is becoming dysfunctional in a fully decarbonized economy (e.g., Khezr and Nepal 2021), because renewable power generation, with its low operating costs, inhibits a sensible price signal. At two, assuming that the market functions regardless, the high level of uncertainty may let investors hesitate rather than invest in new technologies quickly (cf. deep uncertainty in, e.g., Haas et al. 2023).

In this article, we show that both arguments against a market-based approach do not hold and a technology adoption on competitive terms is a viable policy option. For this result, in a first step, we demonstrate that the day-ahead electricity market continues to function even under the condition of a completely decarbonized economy. We show this with a novel market model, in which stochastic processes represent the intermittent supply and demand separately, and verify that the results are robust under a wide range of scenarios. In a second step, we show that in such a market environment, the incentives to invest in electrolyzers without delay are strong enough. In this step, present a generalized method on optimal stopping and show that the so-called option value to wait is negligible.

The remainder of this article is structured as follows. In section two, we introduce our electricity market model. Here, we begin with leveraging recent studies on the ongoing energy transition in Germany. For the resulting parameter space, we develop the stochastic framework for the electricity market. In section three, we describe the optimal stopping methodology for such a market, and suggest an efficient implementation for the numerical simulation. Finally, in section four, we summarize the numerical simulation results, draw conclusions and propose further research. For better readability, most of the data and calculations for sections two and three, as well as the method development for a generalized optimal stopping, are detailed in the appendix.

2. Electricity market model

During the ongoing sustainable energy transition, the electricity market changes fundamentally: conventional power generation is decommissioned, renewable power, mainly wind and solar, is expanded further, and complemented with storage, electrolyzers and backup power. A model with mean-reverting stochastic processes for supply and demand separately is an adequate approach. Such a model does not rely on electricity price time series analyses, which would be insufficient, given the fundamental transformation that we are in. Instead, it allows to use available scenarios on how supply and demand are anticipated to change. Moreover, mean-reverting stochastic processes capture the random aspect of the system well and at the same time, model the typical profiles appropriately with time-dependent trend functions. Lastly, such a setup can be transparently transformed from a state today into an anticipated future, decarbonized state by shifting trends and volatilities. In particular, time-dependent trend functions ensure that seasonal, daily hourly patterns are respected. Further, a suitable selection of the stochastic dynamics ensures that all paths of such a market remain positive. Instead of treating renewable power as a negative demand (e.g., Schöniger and Morawetz 2022), in our model, it is shifting the supply curve whenever renewables are available, to allow for small but positive operating costs of renewables, and the intersection with stochastic demand provides the momentary price. Such a model can be easily calibrated to a base year, in our case the year 2019, and the energy-transition related literature, summarized e.g. in the meta study Wiese et al. (2022), provides the range for supply and demand in a future decarbonized electricity system. Figure 1 displays the future supply curve that we have estimated in this way, on the left in form of generation capacity lined up with its nameplate rating, on the right with dispatchable generation at its rated power and intermittent renewable power added whenever present. The various scenarios are indicated with dotted lines or shades around the base case.

The main parameter groups on the supply side that influence this market model are intermittent and non-intermittent power generation capacity, the share of solar as part of intermittent power and the operating costs. On the demand side, since the level of electrification must be consistent with the supply, price elasticity is the remaining important parameter. By grouping all supply-related parameters for a low, average and high price scenario and by switching demand elasticity from totally inelastic to highly elastic, we span the whole solution space (see table A.3 in the appendix), with a total of 54 scenarios. Consequently, the results show a large variance, displayed in table 1.

While the results vary considerably, as it can be expected in such an uncertain setting combined with a long time horizon, several phenomena prove to be robust when comparing to the base year 2019 in which we had an average price of 37.67 €/MWh in the pricing zone DE_LU and a volatility

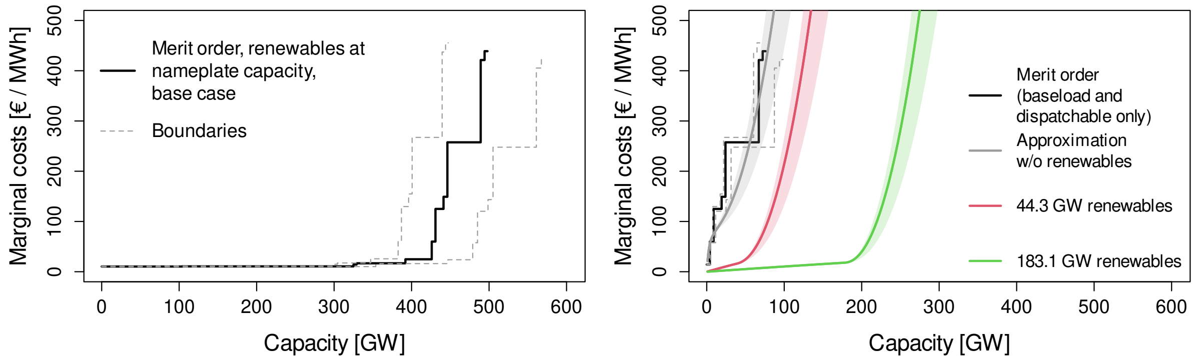

(a) All installed generation capacity with nameplate rating

(b) Baseload and dispatchable capacity with renewables as available

Figure 1: Merit order curve at the end of the time horizon with scenario boundaries

of 12.56 €/MWh[1] (see European Energy Exchange 2023, subscription only). At one, we see that in all scenarios, the average price goes up moderately. While the detail graphs confirm the so-called merit order effect at times when enough renewable power generation is present (for an overview of that topic, see, e.g., Würzburg et al. 2013, or Marshman et al. 2020 for a more recent work), more expensive storage and backup technology offset this effect in average.

Table 1: Expected price and volatility, at the end of time horizon

[€/MWh]		Demand elasticity	
		elastic	inelastic
Expected price	Lower limit	52.0	59.0
	Base case	**69.1 ± 1.3**	**80.8 ± 1.4**
	Upper limit	85.0	98.0
Volatility	Lower limit	28.0	41.0
	Base case	**41.2 ± 1.0**	**59.8 ± 1.1**
	Upper limit	50.0	69.0

At two, the volatility increases. This extends findings in Wozabal et al. (2015), who already link the shape of the supply curve with volatility (ibid, p.6). Our model goes one step further and quantifies this effect. Finally, at three, the model estimates a strong dampening effect of demand elasticity on both average price and volatility. Figure 2 visualizes our market model in form of expected values for the electricity price, complemented with one individual price trajectory, for elastic and inelastic demand, and split into a winter month and a summer month, for the base case.

[1]i.e., the standard deviation of the random part of the electricity price time series

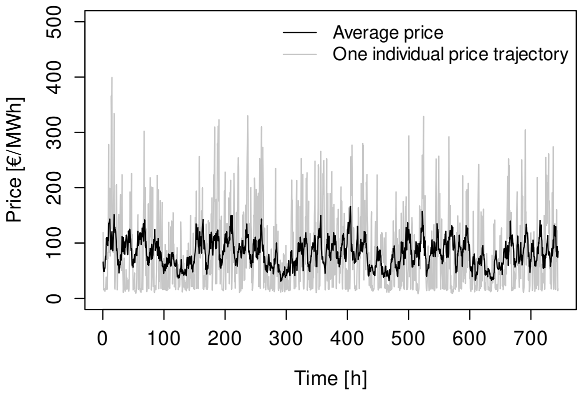

(a) January, inelastic demand

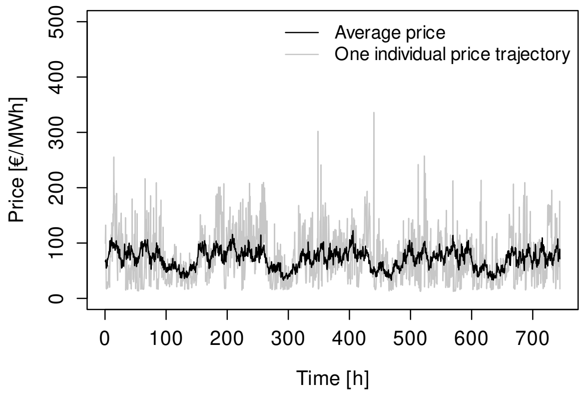

(b) January, elastic demand

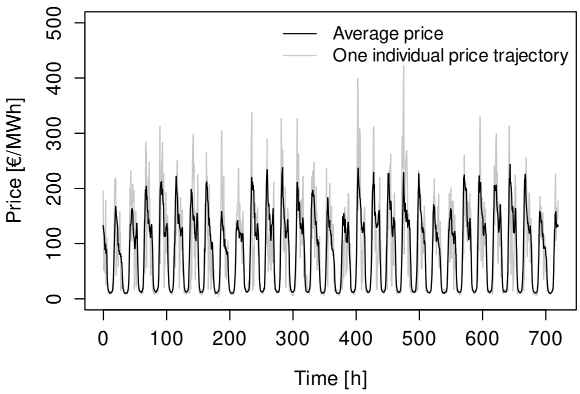

(c) June, inelastic demand

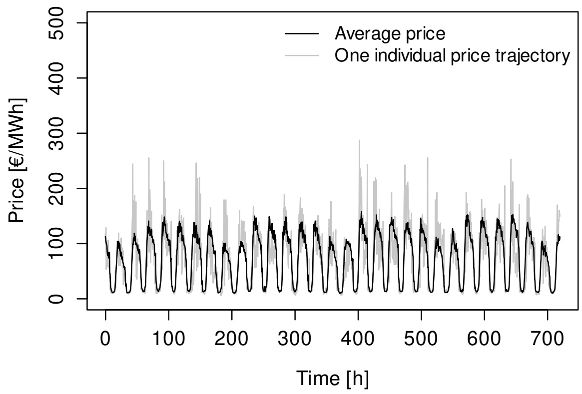

(d) June, elastic demand

Figure 2: Estimated hourly day-ahead prices,
at the end of the transition period, base case

3. Generalized optimal stopping

To complement our market model with the show-case asset, we model a large offshore wind farm with its intermittent production via its random wind resource, similarly to the previously introduced stochastic processes, and transform this into a production with an assumed power curve (see appendix, eq. (B.1)). The electrolyzer itself is modeled with a parameter set that we group into a low-profit, average profit and high-profit electrolyzer definition (appendix, table B.1).

How are investors evaluating such an investment opportunity? There is a particular problem with such an asset, which is common to other new technologies like storage systems and backup power as well. On the one hand, electricity price changes are their business model. With the retrofit implemented, electricity can be sold directly at times of high prices, and at low price times, the operators can optimize their returns and produce hydrogen instead. From a system perspective, this is exactly the desired operating mode as it reacts to both over- and under-supply of electricity. On the other hand, the same price changes may be interpreted as uncertainty and make investors wait. This trade-off can be calculated by treating the investment decision as the right but not the obligation to invest, similar to a financial call option, and calculate the fair value of this option. Hence, we can conclude how in average investors will decide about such a retrofit, once all power generation assets are exposed to fluctuating sales prices.

The method of dynamic programming, in which the payoff function of the investment is modeled as a controlled stochastic process, solves this problem. The controls represent managerial decisions, in our case limited to either wait or invest, and by applying an optimality condition, we find the optimal point in time to stop waiting and to start investing instead. Consequently, at the

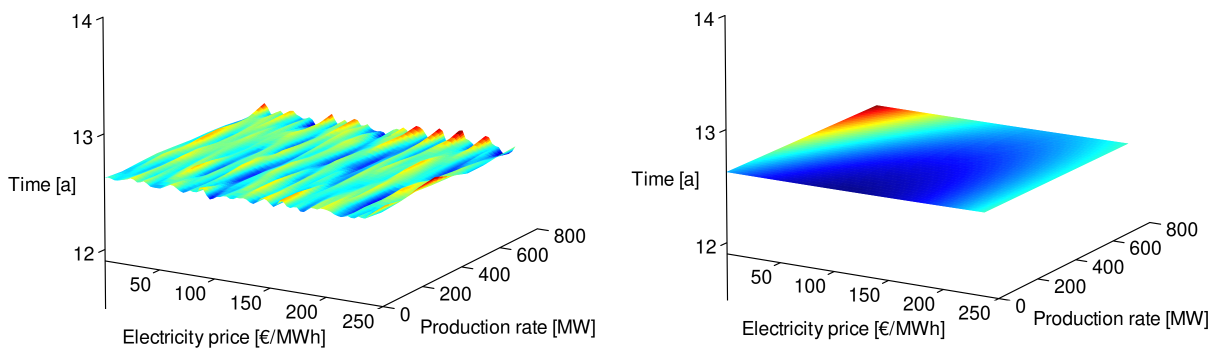

(a) Numerical result

(b) Quadratic regression

Figure 3: Surface that separates waiting from investing

optimal time to invest (i.e., the stopping time), the initial profit function, which is zero in our case, is substituted with the return of the investment itself. In our multidimensional setting, the stopping time creates a surface in the state space spanned by electricity price S_t and wind farm production rate Y_t, and in this way separates the waiting region from the investment region. To the best of our knowledge, it is new to apply dynamic programming to such a general problem. It is common to analyze one-dimensional problems. Further, there are examples of multi-dimensional problems, restricted to quadratic or monotone payoff functions (Christensen et al. 2019 and Christensen and Irle 2020). We run a multi-dimensional problem and do not restrict the payoff function other than being discounted, to not jeopardize the practical relevance of the results. As a consequence, we rely heavily on numerical simulation instead, which we can prove to be computationally efficient nevertheless. For better readability, we have moved this theoretical framework to the appendix B.

A wide range of scenarios must be simulated in order to capture the inherent uncertainty well. To limit the computational effort and still span the complete solution space, we combine a high-price market scenario with a low-profit electrolyzer, an average price scenario with an average profit electrolyzer and a low-price scenario with a high-profit electrolyzer. These three cases are run once with inelastic and once with highly elastic demand. We see that in only two out of six cases, there is a significant incentive to wait – this is the high-price electricity market combined with a low-profit electrolyzer, with no qualitative difference for elastic and inelastic demand. In that case we see that the numerical simulation splits the state space into a waiting region and a region in which investments take place (figure 3). In the regression of the numerical simulation, (figure 3b), we see that there is no relevant curvature the stopping time plane, which is consistent with findings in Schwartz and Smith (2000) – due to the long-term nature of the problem, changes introduced by different starting points do not lead to significant differences in the outcome.

4. Results, conclusion and outlook

Starting with the electricity market, our analysis shows that the market prices are sufficient for financing the investments. The merit order effect is limited to times when there is a high availability of renewable resources and it is offset in average by other technologies. When comparing recent auction results for renewables in Germany (years 2017-2022, wind onshore: 58.4 €/MWh ± 5.0 €/MWh, greenfield photovoltaic: 59.0 €/MWh ± 5.0 €/MWh, see Bundesnetzagentur 2023b and Bundesnetzagentur 2023a), then we see that in all scenarios, the estimated future average prices are sufficient for this power generation segment. For offshore wind, recent auction results are zero and therefore do not provide any indication. However, the feed-in tariff before the year 2017 gave the choice of either 15.4 €-ct/kWh for 12 years or 19.4 €-ct/kWh for 8 years, thereafter 3.9 €-ct/kWh up to year 20 and this leads to an average of 7.5-10.0 €-ct/kWh over the lifetime of 20 years when discounted with interest rates between 1.0-5.0%. This feed-in tariff supported smaller wind turbines with a rotor diameter ≤ 160 m. Therefore, modern turbines with a rotor diameter ≥ 200 m and thus much lower unit costs may also be supported sufficiently well. The next technologies in the merit order curve are storage (batteries, pumped storage hydro and compressed air energy storage, see (figure 1a and table A.2 in the appendix). Here our result shows that as long as batteries do not have to recover their full costs, but instead household and electric vehicle batteries are accessed at their marginal utility for grid operators, their availability can be secured. Next in line is backup power, provided by gas turbines or fuel cells, which are operated with green hydrogen. In the studies we use, their utilization is estimated with ca. 1700 full load hours per year. This is on the same level as for gas fired power stations today (ENTSO-E 2019c and ENTSO-E 2019a), so also in this part of the supply curve, we can conclude that there is sufficient funding. In addition, storage and backup power provide grid services, e.g., frequency and voltage control, which provides additional market-based revenues for this segment. Keles and Dehler-Holland (2022) find that already today, a battery storage system that trades off energy and capacity can generate profits by providing reserve service (tertiary frequency control). Only on the outer most part of the supply curve, there is potentially a problem with refinancing. There we find different variants of biomass, which are placed in this position only due to their high costs, in conflict with their typical operating regime as baseload. Most studies do not see this technology as a major future source of power (exception: Hansen et al. (2019)) and rather see capacity remaining on today's level, so potentially missing re-investment is not such a severe problem. And also here, in combined heat and power applications, like in municipal district heating networks, biomass can still work economically well in a future system. Lastly, our model quantifies the highly positive effect of demand elasticity – its strong dampening effect on both the average price and the volatility becomes clearly visible.

Continuing with the investors' decision making with respect to investments in hydrogen electrolyzers – under the condition that all power generation assets sell via the day-ahead market – only in case of a low-profit electrolyzer operating in a high-price electricity market, the investment does not take place immediately but there's a significant incentive to wait instead. In this case, it takes a long time for the investment to become NPV positive, which is a necessary but not sufficient condition. Then, investors will seek a premium over the defined hurdle rate, which leads to additional waiting. Figure 4b reveals both the premium, at ca. 1.3 %pts, and the additional waiting time of ca. 15 months. Given that this takes place in one of the cases only, we conclude that adopting electrolyzers on competitive terms, without subsidies, is a viable policy option. It requires merely a monitoring of the profitability and potentially a hedging strategy, e.g., in regards

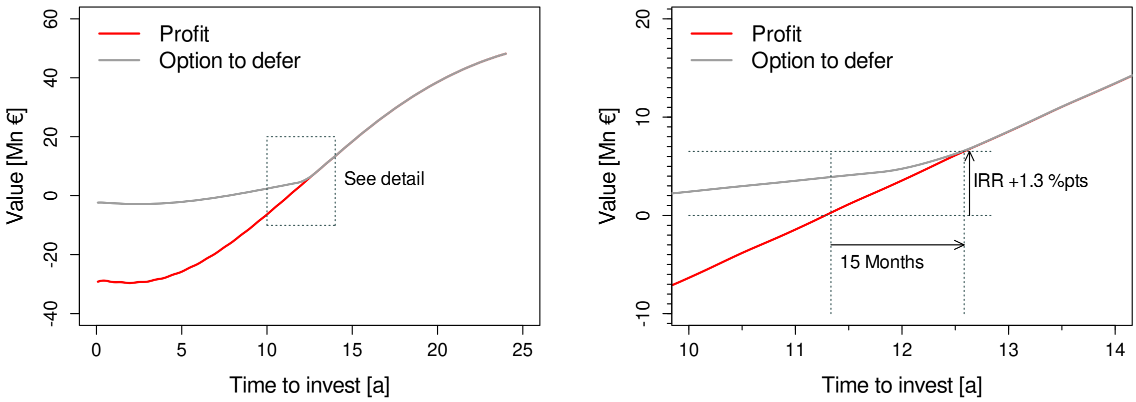

(a) Full time horizon

(b) Zoomed in

Figure 4: Profit as function of time to invest and option value to defer

of the hydrogen price risk, instead of direct subsidies.

With these results in mind, we propose further research on several topics. First, we note that in Germany today, renewable power generation benefits from the privilege of having no relevant price risk. When we remove this privilege, this may reduce the investment volume in this segment as a potential negative side effect. Whether this occurs and to which extent is in our view the main question to clarify before considering the corresponding changes to the market regulation. Further, our market model makes clear how important it will be to use vehicle and household batteries instead of relying on stand-alone installations. Therefore, further work on potential barriers and regulatory fixes in this particular field is crucial for a success of the ongoing sustainable energy transition. Last but not least, the importance of demand elasticity is clearly quantified. First legislative steps have been taken, see Deutscher Bundestag (2023), but additional regulatory activity may be required.

References

BAFA. Bundesamt für Wirtschaft und Ausfuhrkontrolle, Erdgasstatistik. https://www.bafa.de/DE/Energie/Rohstoffe/Erdgasstatistik/erdgas_node.html, 2022. (Accessed on October 10, 2022).

M. T. Barlow. A diffusion model for electricity prices. *Mathematical Finance*, 12(4):287–298, 2002.

Bundesnetzagentur. Solar-Freiflächen, beendete Ausschreibungen. https://www.bundesnetzagentur.de/DE/Fachthemen/ElektrizitaetundGas/Ausschreibungen/

Solaranlagen1/BeendeteAusschreibungen/start.html, 2023a. (Accessed on February 2, 2023).

Bundesnetzagentur. Windenergieanlagen an Land, beendete Ausschreibungen. https://www.bundesnetzagentur.de/DE/Fachthemen/ElektrizitaetundGas/Ausschreibungen/Wind_Onshore/BeendeteAusschreibungen/start.html, 2023b. (Accessed on February 2, 2023).

Sören Christensen and Albrecht Irle. The monotone case approach for the solution of certain multidimensional optimal stopping problems. *Stochastic Processes and their Applications*, 130(4): 1972–1993, 2020. ISSN 0304-4149. doi: https://doi.org/10.1016/j.spa.2019.06.009. URL https://www.sciencedirect.com/science/article/pii/S0304414919303849.

Sören Christensen, Fabián Crocce, Ernesto Mordecki, and Paavo Salminen. On optimal stopping of multidimensional diffusions. *Stochastic Processes and their Applications*, 129(7):2561–2581, 2019. ISSN 0304-4149. doi: https://doi.org/10.1016/j.spa.2018.07.014. URL https://www.sciencedirect.com/science/article/pii/S0304414918303612.

Deutscher Bundestag. Gesetzentwurf zum Neustart der Digitalisierung der Energiewende, Drucksache 20/5549. https://dserver.bundestag.de/btd/20/055/2005549.pdf, 2023. (Accessed on April 25, 2023).

B. Engquist, P. Lötstedt, and B. Sjögreen. Nonlinear filters for efficient shock computation. *Mathematics of computation*, 52:509–537, 1989. ISSN 1088-6842. doi: https://doi.org/10.2307/2008479. URL https://www.ams.org/journals/mcom/1989-52-186/S0025-5718-1989-0955750-9/S0025-5718-1989-0955750-9.pdf.

ENTSO-E. Installed Capacity per Production Type, for Bidding Zone Germany BZN DE-LU. https://transparency.entsoe.eu/generation/r2/installedGenerationCapacityAggregation/show, 2019a. (Accessed on April 9, 2023).

ENTSO-E. Total load - day ahead/actual, for Bidding Zone Germany BZN DE-LU. https://transparency.entsoe.eu/load-domain/r2/totalLoadR2/show, 2019b. (Accessed on October 14, 2023).

ENTSO-E. Actual generation by production type, for Bidding Zone Germany BZN DE-LU. https://transparency.entsoe.eu/generation/r2/actualGenerationPerProductionType/show, 2019c. (Accessed on October 14, 2023).

European Commission. Press Release: The European Green Deal. https://ec.europa.eu/commission/presscorner/detail/en/ip_19_6691, 2019. (Accessed on October, 9, 2023).

European Energy Exchange. EEX Data Server. sftp://eexsftp.drin.aads1.net/

market_data/power/de/spot/csv/, 2023. (Accessed on March 25, 2023, subscription only).

EWI. Gutachterbericht zur dena-Leitstudie Aufbruch Klimaneutralität. https://www.ewi.uni-koeln.de/cms/wp-content/uploads/2022/03/211005_EWI-Gutachterbericht_dena-Leitstudie-Aufbruch-Klimaneutralitaet.pdf, 2021. (Accessed on April 21, 2023).

Christian Haas, Karol Kempa, and Ulf Moslener. Dealing with deep uncertainty in the energy transition: What we can learn from the electricity and transportation sectors. *Energy Policy*, 179:113632, 2023. ISSN 0301-4215. doi: https://doi.org/10.1016/j.enpol.2023.113632. URL https://www.sciencedirect.com/science/article/pii/S0301421523002173.

Lisa Hanny, Jonathan Wagner, Hans Ulrich Buhl, Raphael Heffron, Marc-Fabian Körner, Michael Schöpf, and Martin Weibelzahl. On the progress in flexibility and grid charges in light of the energy transition: The case of germany. *Energy Policy*, 165:112882, 2022. ISSN 0301-4215. doi: https://doi.org/10.1016/j.enpol.2022.112882. URL https://www.sciencedirect.com/science/article/pii/S0301421522001070.

Kenneth Hansen, Brian Vad Mathiesen, and Iva Ridjan Skov. Full energy system transition towards 100% renewable energy in Germany in 2050. *Renewable and Sustainable Energy Reviews*, 102:1–13, 2019. ISSN 1364-0321. doi: https://doi.org/10.1016/j.rser.2018.11.038. URL https://www.sciencedirect.com/science/article/pii/S1364032118307913.

F. Heinz and R. Madlener. Github repository. https://github.com/fheinz01/h2off, 2023. (Accessed on September 28, 2023).

Hersbach et. al. ERA5 hourly data on single levels from 1959 to present. https://cds.climate.copernicus.eu/cdsapp#!/dataset/reanalysis-era5-single-levels?tab=form, 2018. (Accessed on August 12, 2022).

IEA. Global Hydrogen Review. https://www.iea.org/reports/global-hydrogen-review-2023, 2023. (Accessed on June 9, 2024).

ISE. Wege zu einem klimaneutralen Energiesystem. https://www.ise.fraunhofer.de/content/dam/ise/de/documents/publications/studies/Fraunhofer-ISE-Studie-Wege-zu-einem-klimaneutralen-Energiesystem-Update-Klimaneutralitaet-2045.pdf, 2021. (Accessed on October 11, 2023).

I. Karatzas and S.E. Shreve. *Brownian Motion and Stochastic Calculus*. Graduate Texts in Mathematics (Book 113). Springer New York, 1991. ISBN 9780387976556.

Dogan Keles and Joris Dehler-Holland. Evaluation of photovoltaic storage systems on energy markets under uncertainty using stochastic dynamic programming. *Energy Economics*, 106:

105800, 2022. ISSN 0140-9883. doi: https://doi.org/10.1016/j.eneco.2021.105800. URL https://www.sciencedirect.com/science/article/pii/S0140988321006356.

Peyman Khezr and Rabindra Nepal. On the viability of energy-capacity markets under decreasing marginal costs. *Energy Economics*, 96:105157, 2021. ISSN 0140-9883. doi: https://doi.org/10.1016/j.eneco.2021.105157. URL https://www.sciencedirect.com/science/article/pii/S0140988321000621.

P. E. Kloeden and R. A. Pearson. The numerical solution of stochastic differential equations. *The Journal of the Australian Mathematical Society. Series B. Applied Mathematics*, 20(1):8–12, 1977. doi: 10.1017/S0334270000001405.

N.V. Krylov. *Controlled Diffusion Processes*. Stochastic Modelling and Applied Probability. Springer Berlin Heidelberg, 2008. ISBN 9783540709145.

Nicolas Langrené, Geoffrey Lee, and Zili Zhu. Switching to Non-Affine Stochastic Volatility: A Closed-Form Expansion for the Inverse Gamma Model. *Econometrics: Econometric & Statistical Methods - Special Topics eJournal*, 2015.

Daniel Marshman, Michael Brear, Matthew Jeppesen, and Brendan Ring. Performance of wholesale electricity markets with high wind penetration. *Energy Economics*, 89:104803, 2020. ISSN 0140-9883. doi: https://doi.org/10.1016/j.eneco.2020.104803. URL https://www.sciencedirect.com/science/article/pii/S0140988320301432.

National Academy of Science and Engineering. Wasserstoff-Kompass. https://www.wasserstoff-kompass.de/elektrolyse-monitor, 2023. (Accessed on June 7, 2024).

Daniel B. Nelson. ARCH models as diffusion approximations. *Journal of Econometrics*, 45(1): 7–38, 1990. ISSN 0304-4076. doi: https://doi.org/10.1016/0304-4076(90)90092-8. URL https://www.sciencedirect.com/science/article/pii/0304407690900928.

R Core Team. R: A language and environment for statistical computing. https://www.R-project.org/, 2021.

Martin Robinius, Peter Markewitz, Peter Lopion, Felix Kullmann, Chloi Syranidou, Simonas Cerniauskas, Markus Reuß, David Ryberg, Leander Kotzur, Dilara Caglayan, Lara Welder, Jochen Linssen, Thomas Grube, Heidi Heinrichs, Peter Stenzel, and Detlef Stolten. *WEGE FÜR DIE ENERGIEWENDE Kosteneffiziente und klimagerechte Transformationsstrategien für das deutsche Energiesystem bis zum Jahr 2050*. Forschungszentrum Jülich, July 2020. ISBN 978-3-95806-483-6.

Timothy Sauer. Computational solution of stochastic differential equations. *Wiley Interdisciplinary Reviews: Computational Statistics*, 5, 2013.

Eduardo Schwartz and James Smith. Short-term variations and long-term dynamics in commodity prices. *Management Science*, 46:893–911, 07 2000. doi: 10.1287/mnsc.46.7.893.12034.

Franziska Schöniger and Ulrich B. Morawetz. What comes down must go up: Why fluctuating renewable energy does not necessarily increase electricity spot price variance in Europe. *Energy Economics*, 111:106069, 2022. ISSN 0140-9883. doi: https://doi.org/10.1016/j.eneco.2022.106069. URL https://www.sciencedirect.com/science/article/pii/S0140988322002353.

R.H. Shumway and D.S. Stoffer. *Time Series Analysis and Its Applications: With R Examples*. Springer Texts in Statistics. Springer International Publishing, 2017. ISBN 9783319524528.

W. Shyy, M.-H. Chen, R. Mittal, and H.S. Udaykumar. On the suppression of numerical oscillations using a non-linear filter. *Journal of Computational Physics*, 102(1):49–62, 1992. ISSN 0021-9991. doi: https://doi.org/10.1016/S0021-9991(05)80004-X. URL https://www.sciencedirect.com/science/article/pii/S002199910580004X.

Maciej M. Sokołowski and Raphael J. Heffron. Defining and conceptualising energy policy failure: The when, where, why, and how. *Energy Policy*, 161:112745, 2022. ISSN 0301-4215. doi: https://doi.org/10.1016/j.enpol.2021.112745. URL https://www.sciencedirect.com/science/article/pii/S030142152100611X.

Frauke Wiese, Johannes Thema, and Luisa Cordroch. Strategies for climate neutrality. Lessons from a meta-analysis of German energy scenarios. *Renewable and Sustainable Energy Transition*, 2:100015, 2022. ISSN 2667-095X. doi: https://doi.org/10.1016/j.rset.2021.100015. URL https://www.sciencedirect.com/science/article/pii/S2667095X21000155.

David Wozabal, Christoph Graf, and David Hirschmann. The effect of intermittent renewables on the electricity price variance. *OR Spectrum*, 03 2015. doi: 10.1007/s00291-015-0395-x.

Klaas Würzburg, Xavier Labandeira, and Pedro Linares. Renewable generation and electricity prices: Taking stock and new evidence for Germany and Austria. *Energy Economics*, 40:S159–S171, 2013. ISSN 0140-9883. doi: https://doi.org/10.1016/j.eneco.2013.09.011. URL https://www.sciencedirect.com/science/article/pii/S0140988313002065. Supplement Issue: Fifth Atlantic Workshop in Energy and Environmental Economics.

Yu Zhang, Qingsheng Li, Yeyan Xu, Liangzhong Yao, Fan Cheng, and Yunxin Liu. Marginal utility of battery energy storage capacity for power system economic dispatch. *Energy Reports*, 8:397–407, 2022. ISSN 2352-4847. doi: https://doi.org/10.1016/j.egyr.2022.09.120. URL https://www.sciencedirect.com/science/article/pii/S2352484722018443. The 2022 International Conference on Energy Storage Technology and Power Systems.

Appendix A. Electricity market model

The current electricity system is quantified in detail in the databases ENTSO-E (2019b), ENTSO-E (2019a) and ENTSO-E (2019c). The high-resolution data therein provide hourly load profiles and so, provide the stochastic distribution parameters for renewable supply and total demand. Scenarios for a future electricity system can be found in the literature. Here, ref. Wiese et al. (2022) provides an overview of relevant studies for the German market place. Among these, Robinius et al. (2020) provides an average scenario[2], and the other studies that are created in academic institutions (Hansen et al. 2019, EWI 2021 and ISE 2021) are used to cross-check and to define the upper and lower limits for the relevant parameters. With this information, we scale up the electricity system (appendix, table A.1) and estimate operating costs (appendix, table A.2). With data on gas consumption for heating in the building sector today (BAFA 2022), and with an analysis of the seasonal consumption pattern of electric vehicles (Zhang et al. 2022), we adapt further the seasonal pattern of the electricity demand. Back to the supply side, the future volatility is be

Table A.1: Generation and storage capacity by type in year 2050
base case, in descending order

Technology	Capacity	
	[GW]	[%]
Onshore wind	221.0	44
PV - greenfield	104.0	21
PV - rooftop	63.0	13
Fuel cells, gas turbines	43.0	
Offshore wind	34.0	
Pumped storage hydro	10.4	
Compressed air energy storage	5.0	
Biomass (gas)	5.0	
Batteries	4.8	
Run-of river hydro	4.0	
Biomass (solid)	3.8	
Total	498.0	

Sources: Robinius et al. (2020), pp. 4, 25-28, 31-33
ENTSO-E (2019a)

found by scaling up today's volatility such that the full-load hours for renewable power generation that are estimated in the aforementioned studies are met. To make use of these forecasts, we have

[2]In regards to this study, we always refer to the scenario S95, i.e., 95% CO_2 reduction, including preparations for dark doldrums.

Table A.2: Operating costs in year 2050
base case, in ascending order

Technology	Operating costs [€/kWh]
PV - greenfield	0.010
Onshore wind	0.011
Run-of-river hydro	0.014
PV - rooftop	0.017
Offshore wind	0.025
Batteries (marginal utility)	0.060
Pumped storage hydro	0.125
Compressed air energy storage	0.149
Fuel cells and Gas turbines	0.258
Biomass (gas)	0.421
Biomass (solid)	0.439
Batteries (full costs)	4.130

Sources: Robinius et al. (2020), pp. 28, 32, 103ff; Zhang et al. (2022), ENTSO-E (2019c), ENTSO-E (2019a); own calculations

Table A.3: Scenario definition – relative to the average, at the end of the time horizon

No	Dimension	Lower	Base	Upper
1	Generation capacity and demand			
	Intermittent generation	97%	100%	103%
	Non-intermittent generation	90%	100%	130%
2	Share of solar capacity	30%	40%	50%
3	Operating costs	96%	100%	104%
4	Demand elasticity	Elastic or inelastic		

developed the following two-dimensional electricity price model, by extending a model from Barlow (2002). We use stochastic mean-reverting processes and model supply and demand patterns separately, with time-dependent periodic trend functions, and ensure positive paths for supply and demand by changing from a normal distribution to a so-called Inverse Gamma dynamics:

$$dX_t = \Theta(\mu(t) - X_t)dt + \tilde{\sigma} X_t dW_t \,. \tag{A.1}$$

Here, $X_t = (X_t^{(1)}, X_t^{(2)})$ is the two-dimensional stochastic process which models renewable supply in its first and total demand in its second component, dW_t is a two-dimensional Brownian motion, and finally, volatility σ and mean-reversion parameter Θ are diagonal matrices. The trend function $\mu(t) = (\mu^{(1)}(t), \mu^{(2)}(t))$ represents the seasonal trend for renewable power generation (solar PV and wind, on- and offshore) in its first component and the load profile of the total demand in its second component. For calibrating the profiles, it is sufficient to use linear combinations of periodic functions for the trends. Under this restriction and at first using a normal distribution dynamics, a simple estimate shows that the expected value converges to the trend, as it is desired. The equations are globally Lipschitz and growth limited, so with Karatzas and Shreve (1991), p.289, we can show that this holds true for an Inverse Gamma dynamics, too. Further, the references Langrené et al. (2015) and Nelson (1990) show the positivity of paths, which holds also in the two-dimensional setup. And lastly, they show how the standard deviation, measured in the empirical data and denoted σ, corresponds to the volatility of the dynamics $\tilde{\sigma}$:

$$\tilde{\sigma}_i = \sigma_{X^{(i)}} \sqrt{\frac{2\,\Theta_{ii}}{(\mu^{(i)})^2 + \sigma^2_{X^{(i)}}}}\,, \qquad i = 1, 2\,.$$

The regressions for the trends are found with spectral analysis of the empirical data in the base year. The seasonal cycle for wind is

$$\mu_1^{(1)}(t) \;=\; 14217.9 + 5736.9\cos\left(\frac{2\pi t}{8760}\right) + \; 1315.2\sin\left(\frac{2\pi t}{8760}\right), \qquad t \text{ in hours.}$$

The daily and seasonal cycle for solar is

$$\begin{aligned}\mu_2^{(1)}(t) \;=\; & \left(1 + 0.9\cos\left(\frac{2\pi t}{8760} + 3.3\right)\right) \\ & \cdot \left(4799.1 + \sum_{i=1}^{4} C_i \cos\left(\frac{2\pi\omega_i t}{8760}\right) + \sum_{i=1}^{4} D_i \sin\left(\frac{2\pi\omega_i t}{8760}\right)\right)\end{aligned}$$

with its coefficients given in table A.4. The complete trend for the supply side is the sum of both.

Table A.4: Coefficients for the daily pattern in solar production, year 2019

i	Time per cycle [h]	Coefficient C_i	D_i
1	24	-7419.1	512.2
2	12	3132.6	-492.4
3	8	-323.6	150.8
4	6	-272.5	39.3

On the demand side, we have the following seasonal cycle:

$$\mu_1^{(2)}(t) = 59966.0 + 3805.9 \cos\left(\frac{2\pi t}{8760}\right) + 730.2 \sin\left(\frac{2\pi t}{8760}\right) \quad \text{in [MW]}.$$

In addition, we have an hourly cycle as follows:

$$\mu_2^{(2)}(t) = \sum_{i=1}^{11} A_i \cos\left(\frac{2\pi\omega_i(t-72)}{672}\right) + \sum_{i=1}^{11} B_i \sin\left(\frac{2\pi\omega_i(t-72)}{672}\right)$$

with its coefficients given in table A.5. They are determined with data from February 2019 in order to avoid holidays, which considerably complicate the regression without adding any useful information. We scale the trend functions such that at time $t = 0$, they represent the base year, and

Table A.5: Coefficients for the weekly and daily periodic fit

i	Frequency cycles / 4 weeks	Coefficient A_i	B_i
1	4	2157.5	-5942.4
2	8	2799.8	2641.6
3	12	-1326.5	-
4	16	1061.1	-
5	20	-1320.7	1086.1
6	24	-531.8	-1476.2
7	28	-7452.5	-3724.8
8	32	-	976.4
9	56	-1657.6	-3964.6
10	60	-448.1	603.2
11	112	700.9	646.8

at the end of the time horizon, they represent one of the scenarios defined. The calculations are carried out in R (see R Core Team 2021), the spectral analysis is explained in, e.g., Shumway and Stoffer (2017).

The price is modeled as a function of supply and demand, by using

$$F(x_1, x_2) = c_2 \arctan\left(\frac{x_2}{c_1 + c_4 x_1}\right) + c_3 \left(1 + \alpha \frac{x_2 - x_1}{c_1}\right)^{1/\alpha}.$$

Variable x_1 represents renewable power supply, x_2 represents total demand. The first summand provides marginal costs for renewable power generation, whenever renewable power resources are available. The second summand models the dispatchable power generation, i.e., conventional power generation in the base year, and a collection of storage and backup power in the future. The parameters α and c_i are used to calibrate the model to the base year 2019 at first, and secondly, when turned into time-dependent linear functions, they transform the supply curve from the base year into a future supply curve. The electricity price finally is

$$S_t^E = F_{\alpha, c_i}(X_t^{(1)}, X_t^{(2)}, t) \tag{A.2}$$

This model can be solved numerically. Here, a backward test shows that the resolution in the time axis must be as small as 30 min because of the steep changes in the trend functions. This, in combination with the long time horizon, leads to a high computational effort, which at first we counter with an efficient two-step algorithm for integrating the differential equations (see Kloeden and Pearson 1977 or Sauer 2013) and second, by implementing it with a high-performance compiler, here C++. The table A.3 defines 54 scenarios, which we calculate numerically and this yields the ranges for expected future electricity price and volatility, presented in table 1 in the main part of this article.

Appendix B. Generalized optimal stopping

Equation (A.2) can be expanded to

$$\begin{aligned} dS_t^E &= \frac{\partial F}{\partial t}(t, X_t)\,dt + \nabla F(t, X_t)\,dX_t + \frac{1}{2}\,\Sigma_{i,j=1}^2 \frac{\partial^2 F}{\partial x_i \partial x_j}(t, X_t)\,d[X^{(i)}, X^{(j)}]_t \\ &= \left(\frac{\partial F}{\partial t} + \frac{1}{2}\left(\frac{\partial^2 F}{\partial x_1^2}\sigma^2_{X^{(1)}} X_t^{(1)} + \frac{\partial^2 F}{\partial x_2^2}\sigma^2_{X^{(2)}} X_t^{(2)}\right) + \nabla F\,\Theta\,(\mu(t) - X_t)\right) dt + \nabla F \sigma\,dW_t \\ &= S_1(t, X_t)\,dt + S_2(t, X_t)\,dW_t \quad \text{a.s.} \end{aligned}$$

which provides the first set components for the optimal stopping problem.

For the electrolyzer to be analysed, we first define a wind farm with its wind resource Q_t and a power curve P that converts wind into an electricity production rate Y_t, in the same manner as before:

$$dQ_t = \zeta\,(\kappa(t) - Q_t)\;dt + \tilde{\sigma}_Q(t)Q_t\,dW_t\,, \qquad Y_t = P(Q_t)\,. \tag{B.1}$$

Trend, mean-reversion parameter and volatility are found with the same methods as for the electricity market, this time using climatic data from Hersbach et. al. (2018). Hence,

$$\begin{aligned} dY_t(Q_t) &= \frac{\partial P}{\partial x}(Q_t)\,dQ_t + \frac{1}{2}\frac{\partial^2 P}{\partial x^2}(Q_t)\,\sigma_Q^2 dt \\ &= \left(\frac{\partial P}{\partial x}(Q_t)\zeta\,(\kappa(t) - Q_t) + \frac{\sigma_Q^2}{2}\frac{\partial^2 P}{\partial x^2}(Q_t)\right)dt + \sigma_Q\,\frac{\partial P}{\partial x}(Q_t)\,dW_t \\ &= Y_1(t, Q_t)\,dt + Y_2(t, Q_t)\,dW_t \quad \text{a.s.} \end{aligned}$$

provides the remaining components for the stopping problem. For the payoff function, we model the electrolyzer as follows. Let S^{H_2} be the hydrogen price, η the electrolyzer efficiency, I the investment expenditure, C the variable costs of operation, and M the fixed costs of operation (without capital costs). Then,

$$\pi_t = \begin{cases} Y_t\,(S^{H_2}\eta - S_t^E - C) & \text{for } S_t^E < S^{H_2}\eta - C \\ 0 & \text{otherwise} \end{cases}$$

is the gross profit rate (regularized and assumed differentiable going forward). Like in the electricity market model, the average values for S^{H_2}, η and C are taken from Robinius et al. (2020), and the references ISE (2021), EWI (2021) and Hansen et al. (2019) are used as cross-check or for defining upper and lower limits (table B.1). The sources estimate changes in these parameters over time, which is reflected as well. The momentary value of such an investment project is

$$v_t = \pi_t - M = \pi(Y_t, S^{H_2}, S_t^E(t, X_t)) - M(t)\,.$$

For formal reasons, the explicit time dependency in the equations above is moved to a third stochastic process Z_t that follows the equation $dZ_t = dt$ and we summarize this as

$$d\Gamma_t = B(\Gamma_t)dt + \Lambda(\Gamma_t)dW_t\,,$$

with $\Gamma_t = (S_t^E, Y_t, Z_t)$, $B \in \mathbb{R}^3$, $\Lambda \in \mathbb{R}^{3\times 2}$ and W_t being a two-dimensional Brownian motion[3].

[3]For easier reading, we sometimes denote $(S_t, Y_t, Z_t) = (x, y, z)$ or $= (x, y, t)$.

Table B.1: Parameters for the electrolyzer, values at the start and end of the time horizon

Parameter		Profitability scenario			Unit
		Low	Average	High	
Investment expenditure	Start	1450	1350	1250	[€/MWh]
	End	540	500	460	
Operation and maintenance	Start	43	40	37	[€/MW, a]
	End	16	15	14	
Efficiency	Start	63	65	67	[%]
	End	68	70	72	
Hydrogen sales price		121	124	127	[€/MWh]

Figures rounded; sources: Robinius et al. (2020), Hansen et al. (2019), ISE (2021), EWI (2021)

We let $v^{(u)}(\Gamma_t)$ denote the momentary value of such an investment at a certain point Γ_t in our state space, controlled by a control strategy u (i.e., a sequence of managerial decisions) and then have, for one chosen control strategy u_t, the value of the investment over the complete time horizon:

$$v^{(u)}(\Gamma_0) = \int_0^\infty v^{(u_t)}(\Gamma_t)\, dt\,,$$

with starting point Γ_0. Finding an optimal control means solving

$$V(\Gamma_0) = \sup_u \left\{ V^{(u)}(\Gamma_0) \right\} = \sup_u \left\{ E\left[\int_0^\infty v^{(u_s)}(\Gamma_s) ds \right] \right\} . \tag{B.2}$$

We restrict the control process u_t to stopping, i.e., to a pair of value functions v_1 and v_2 and the fact that before the stopping time t^*, the value is accrued via v_1 and after stopping, this is taken over by v_2. According to Belmann's principle of optimization, this changes (B.2) to

$$V(\Gamma_0) = \sup_{t^*} \left\{ E\left[\int_0^{t^*} v_1(\Gamma_s) ds + v_2(\Gamma_{t^*}) \right] \right\} ,$$

which simplifies further since before stopping, investors are just waiting, without generating any value ($v_1 \equiv 0$). Additionally, we restrict v_2 to functions of the form $g \exp(-\rho t)$. With Krylov (2008), p.13, with above restrictions, the optimal stopping problem turns to solving

$$v_2 - V + \left[\nabla V B + (1-\rho) V + \frac{1}{2}\left(\Lambda_{11}^2 \frac{\partial^2 V}{\partial x^2} + \Lambda_{22}^2 \frac{\partial^2 V}{\partial y^2} \right) - v_2 \right]_+ = 0\,.$$

Here, $[x]_+ = 1/2(x + |x|)$ takes the positive part of the interior. This equation can be solved by iterating the operator

$$\Phi(V) := v_2(\Gamma_0) + \Bigg[B_1(\Gamma_0)\frac{\partial V}{\partial x}(\Gamma_0) + B_2(\Gamma_0)\frac{\partial V}{\partial y}(\Gamma_0) + \frac{\partial V}{\partial t}(\Gamma_0) + (1-\rho)V(\Gamma_0) + \frac{1}{2}\left(\Lambda_{11}^2(\Gamma_0)\frac{\partial^2 V}{\partial x^2}(\Gamma_0) + \Lambda_{22}^2(\Gamma_0)\frac{\partial^2 V}{\partial y^2}(\Gamma_0)\right) - v_2(\Gamma_0)\Bigg]_+ \quad \text{for all } \Gamma_0.$$

on a start function V_0. For solving numerically, we define again the stopping time t^* as being the smallest time such that $V(S_t^E, Y_t, t) \geq v_2(S_t^E, Y_t, t)$ for $0 \leq t \leq t^*$ ($t^* = 0$ or $t^* = \infty$ possible), and we define the continuation region $C = \{\Gamma \in \mathbb{R}^2 \times [t^*, \infty) \,|\, V(\Gamma) \geq v_2(\Gamma)\}$. Next, we define the set A as the closure of $\mathbb{R}^2 \times [0, \infty) \cap \{Y > 0\}$. Here, any such set fulfills the necessary and sufficient criterion for solvability, which is that for all $x \in A$, a number $\delta > 0$ shall exist such that $(\Lambda\Lambda^{\text{tr}} x)x \geq \delta$ (ibid, pp.203 ff). This holds true because for our class of problems, $\Lambda\Lambda^{\text{tr}}$ is positive semi-definite and positive definite when projected into the subspace $\mathbb{R}^2$. Thus, the value of waiting V is given by

$$\lim_{n\to\infty} \Phi^n(V(\Gamma)) = V(\Gamma) \quad \text{for} \quad \Gamma \in A \cap C,$$

which can be approximated numerically by iterating the operator Φ in difference form on a discretized state space, with an appropriately chosen start function V_0.

Figure B.5 displays a possible object-oriented architecture; for an actual implementation and further explanatory documents, see Heinz and Madlener 2023. For the operator iteration, it is important to note that from the numerical analysis of partial differential equations, the phenomenon of spurious oscillations is known (e.g., Shyy et al. 1992). We apply the common solution to this problem of, at first, increasing the resolution as much as possible and, second, by iterating and filtering in an alternating sequence with a conservation law filter (cf. Engquist et al. 1989).

To keep the calculation time under control, out of the 54 scenarios from the market model, the low, average and high-price case are selected. The parameters which define the asset performance are grouped into defining a low, average and high profitability electrolyzer. Then, in order to identify the complete span of possible results, the market scenario with a high electricity price is combined with a low-profitability electrolyzer, the low electricity price is combined with a highly profitable electrolyzer, and the average market scenario is combined with a medium profitability electrolyzer. These three combinations are calculated once for inelastic and highly elastic demand, and in that way, we manage to represent the full set of potential results with a number of iterations as small as possible.

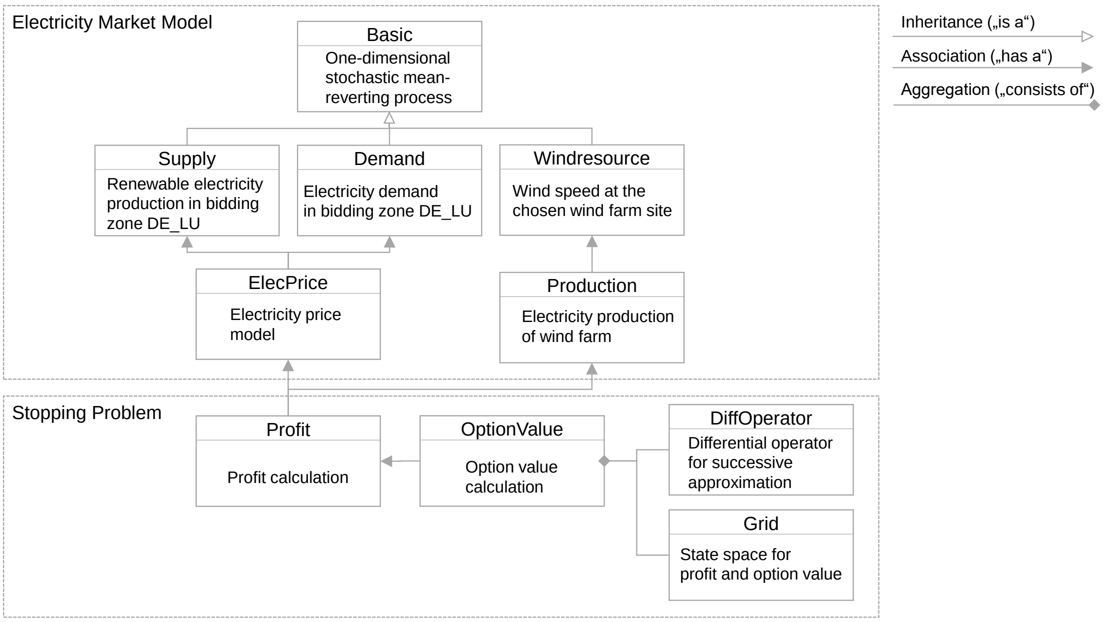

Figure B.5: Proposed class diagram for implementation